

Parking assistance system for leaving perpendicular parking lots: experiments in daytime/nighttime conditions

D. F. Llorca, I. G. Daza, S. Álvarez, A. M. Hellín, M. A. Sotelo

Abstract—Backing-out and heading-out maneuvers in perpendicular or angle parking lots are one of the most dangerous maneuvers, specially in cases where side parked cars block the driver view of the potential traffic flow. In this paper a new vision-based Advanced Driver Assistance System (ADAS) is proposed to automatically warn the driver in such scenarios. A monocular gray-scale camera was installed at the back-right side of a vehicle. A Finite State Machine (FSM) defined according to three CAN-Bus variables and a manual signal provided by the user is used to handle the activation/deactivation of the detection module. The proposed oncoming traffic detection module computes spatio-temporal images from a set of pre-defined scan-lines which are related to the position of the road. A novel spatio-temporal motion descriptor is proposed (STHOL) accounting the number of lines, their orientation and length of the spatio-temporal images. Some parameters of the proposed descriptor are adapted for nighttime conditions. A Bayesian framework is then used to trigger the warning signal using multivariate normal density functions. Experiments are conducted on image data captured from a vehicle parked at different locations of an urban environment, including both daytime and nighttime lighting conditions. We demonstrate that the proposed approach provides robust results maintaining processing rates close to real-time.

Index Terms—Park Assist, Perpendicular and Angle Parkings, Backing-out Maneuvers, Spatio-temporal Images, Motion Patterns, ADAS, Daytime, Nighttime.

I. INTRODUCTION

In the last years, a considerable number of research works and industrial developments on Intelligent Parking Assist Systems (IPAS) have been proposed, including both assistance and automatic parking approaches. Most of these systems have been designed to assist the driver when parking in parallel, perpendicular or angle parking lots. However the development of intelligent systems designed to assist the driver when leaving the parking lots has been somewhat neglected in the literature.

The nature of parking assistance systems for entering a parking lot is different from that of parking assistance systems for backing-out manoeuvres. On the one hand, the main goal of IPAS that assist drivers when parking is to ease the maneuver avoiding small collisions, reducing car damage, and avoiding personal injuries. Although the number of injured people is not negligible at all (more than 6.000 people are injured yearly by vehicles that are backing up only in the United States [1]), the

low speed of the vehicles involved in the accidents reduce the severity of the damage. On the other hand, leaving parking manoeuvres imply to enter in an active traffic lane where vehicles move at a relative speed much higher than the speed of the vehicle that is leaving the parking lot. This situation can be particularly dangerous when the pull out manoeuvre has to be done blindly, since the driver does not have visibility of the oncoming traffic. In other words, the safety component of IPAS devised to assist the driver when leaving a parking space is much more relevant since the possible collisions may cause serious injuries and damages.

In this paper we present an extended version of our previous work [2] that includes experiments in nighttime conditions. The new vision-based Advanced Driver Assistance System (ADAS) was designed to deal with scenarios like the ones depicted in Figs. 1(a)-1(d). We consider backing-out or heading-out maneuvers in perpendicular or angle parking lots, in cases where side parked cars block the driver view of the potential traffic flow. In such scenarios the common recommendation can be simplified as to move slow looking at every direction, but it is not possible to avoid initiating the maneuver in blind conditions. We propose a vision-based solution using a camera located at the back-right side of the vehicle which captures images with a better Field of View (FOV) than the driver's FOV (see Fig. 1). Note that the same solution can be easily extended for heading-out maneuvers by installing the camera at the front-left side of the vehicle.¹

We propose a probabilistic model of the spatio-temporal motion patterns obtained from a set of virtual lines placed following the road location. The spatio-temporal domain is analyzed by accounting the number of lines and their length with respect to their orientations in a histogram of orientations that we so-called Spatio-Temporal Histograms of Oriented Lines (STHOL). The resulting feature vectors are modeled assuming a normalized multivariate Gaussian distribution for two types of scenarios (classes): *oncoming traffic* and *free road*. Bayes decision theory is then used by means of discriminant functions based on the minimum error rate that assumes equal prior probabilities. Finally, if the p.d.f. of the *oncoming traffic* class is larger than *free traffic* class p.d.f, the system triggers a warning signal that alerts the driver of oncoming traffic.

The remainder of this paper is organized as follows: the state of the art is discussed in Section II. In Section III the general

D. F. Llorca, I. G. Daza, S. Álvarez, A. M. Hellín, M. A. Sotelo are with the Computer Engineering Department, Polytechnic School, University of Alcalá, Madrid, Spain. email: llorca, sergio.alvarez, sotelo@aut.uah.es.

¹In countries with left-hand traffic the cameras will be located at the back-left/front-right sides of the vehicle.

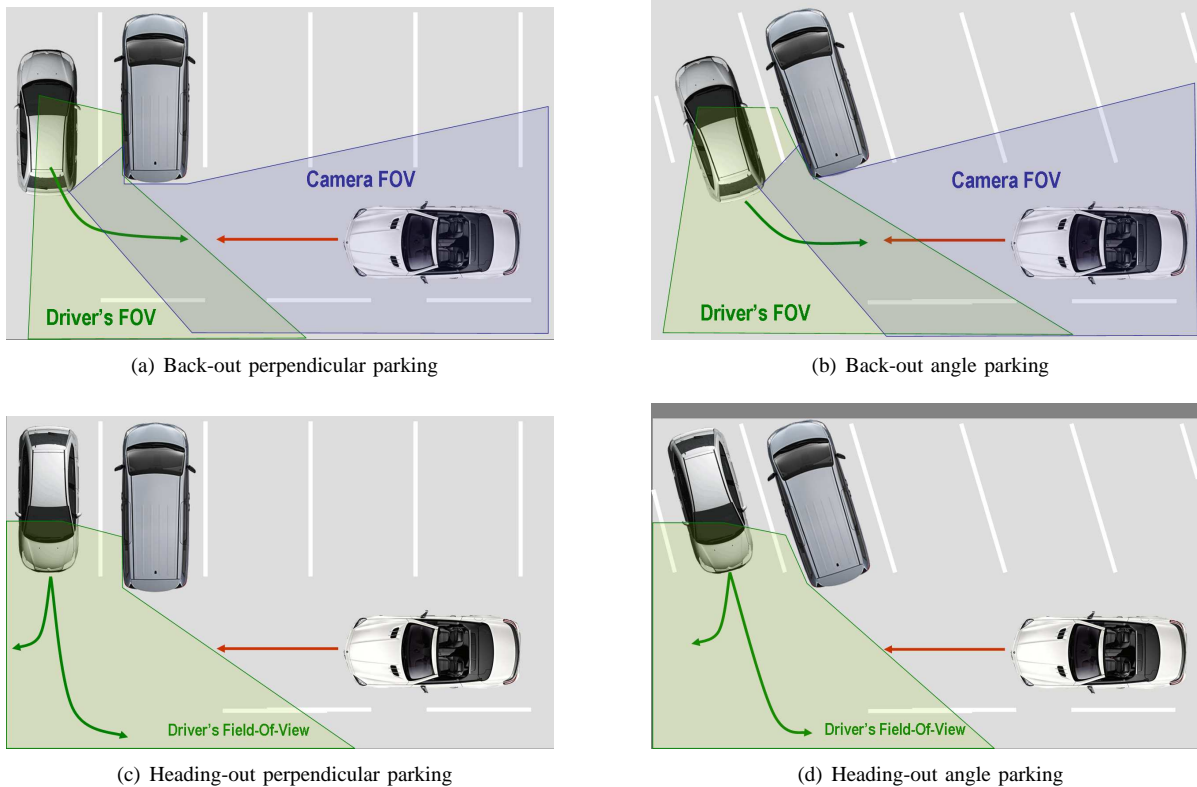


Fig. 1. Driver and camera Field of View (FOV) in countries with right-hand traffic.

and global structure of the system is described. Section IV introduces the spatio-temporal detection model including the feature descriptor and the Bayesian decision scheme. Section V serves to evaluate the performance of the system in both daytime and nighttime conditions. Finally, in Section VI we present the conclusions and future work.

II. RELATED WORK

A sizeable body of literature exists related to IPAS, including range sensor-based approaches [3], monocular-based systems [4], [5], and motion stereo-based proposals [6]. However all these systems propose target position-designation methods to assist the driver when parking or to perform automatic parking. The closest field related with our proposal can be found in the area of Blind Spot Detection systems (BSD) that monitor the road behind and next to the host vehicle, warning the driver when there are vehicles in the blind spot of the side-view. These systems are mainly based on the use of cameras installed in the left and/or right door mirrors [7]. These systems can be utilized to assist the driver when leaving a parallel parking lot, but the position of the camera makes not possible to use BSD systems in the scenarios depicted in Fig. 1. In addition, BSD systems usually take advantage of the opposite direction between the implicit optical flow and the motion of the overtaking vehicles. This difference is not so evident in the scenarios used in this work.

Considering the recognition of vehicles in the context of ADAS, extensive literature is available for both forward and rear vehicle detection [8]. The FOV of the camera and the type

of maneuver when leaving a perpendicular or angle parking (see Fig. 1) provide images similar to the ones used by rear vehicle detection systems [9]. Most of these systems follow a three-staged framework: Region-Of-Interest (ROI) generation (monocular or stereo [10]), classification and tracking. All these stages are needed since the system has to deal with a wide number of scenarios and driving conditions. However, in the context of our application, the number of possible scenarios is much lower so we aim to devise a simpler system without this tree-staged scheme.

III. SYSTEM DESCRIPTION

The proposed architecture of the system is composed of three main parts: camera, processor and CAN-Bus communications. A gray-scale 640×480 resolution camera is used, with a focal length of $12.5mm$. The location of the camera is depicted in Fig. 2. This is obviously a preliminary structure since the camera should be integrated inside the vehicle bodywork. As can be observed in Figs. 3(a) and 3(b) the point of view of the camera is much better than the driver's point of view.

The processor is a PC-based architecture that is connected with both the camera and the CAN-Bus interface. From the CAN-Bus we obtain the following variables: *steering angle*, *car speed* and *current gear*. These variables are used to trigger on/off the detection module according to the Finite State Machine (FSM) described in Fig. 4. As can be observed the system has to be firstly activated by the user. Then the system waits until the car has been put into reverse gear and the



Fig. 2. Camera located at the back-right side of the vehicle.



(a) Driver's point of view (b) Image captured by the camera

Fig. 3. Driver and camera point of view.

detection module is then triggered on. The system stops if one of the following conditions are met: (1) vehicle speed is greater than 5km/h or (2) steering angle is greater than 10 degrees with respect to the zero reference position or (3) reverse gear is deactivated.

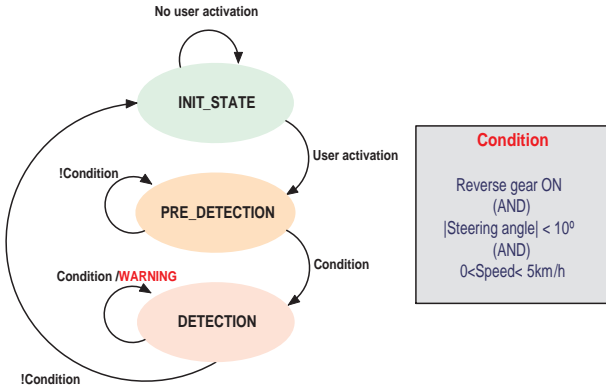


Fig. 4. FSM for detection module.

IV. SPATIO-TEMPORAL DETECTION MODEL

An overview of the proposed spatio-temporal detection model of the oncoming traffic is depicted in Fig. 5. Spatio-temporal images are computed using a pre-defined grid of scan-lines which are related with the location of the road. These images are then analyzed using a line detection stage, which provides the lines, their orientation and length. This information is used to compute the so-called Spatio-Temporal Histograms of Oriented Lines (STHOL), which are the features used to represent the current state of the adjacent lane:

oncoming traffic or free traffic. Finally, a Bayesian decision scheme is used to trigger the warning signal to the user, that can be a simple acoustic tone or a more sophisticated user interface.

The proposed approach can be used in either daytime and nighttime conditions. A specific module has been designed to assess the lighting conditions of the images captured by the camera. The different lighting conditions are roughly divided in two modes of operation: daytime and nighttime. As in [11], the average intensity of the image and the density of gradients are used to decide when nighttime processing begins and daytime processing stops. The main differences between both modes are related with the set of parameters used in the line detection stage, and the likelihoods applied in the Bayesian decision scheme. Thus, we maintain the same structure for both daytime and nighttime scenarios, which constitutes a clear contribution since most of the vision-based vehicle detection systems clearly differs in their architecture depending on the lighting conditions [8], [11].

In the following, details of each one of the modules represented in Fig. 5 are given.

A. Spatio-temporal images

Vehicle detection proceeds with the computation of spatio-temporal images which represents a single intensity scan-line collected over several frames. This approach was presented in [12] to perform crowd detection in video sequences using a set of horizontal scan-lines. In our case, the distribution of the scan-lines follows a pre-defined representation of the road using the flat world assumption, extrinsic parameters of the camera w.r.t. the road (obtained by means of an off-line camera calibration process) and a pre-defined grid which covers half of the road. The definition of the number of scan-lines and their distribution have been experimentally determined taking into account the maximum and minimum range, the orientation of the camera as well as a trade-off between computation time and the density of information. Some examples are depicted in Figs. 6(a)-6(d) for both daytime and nighttime conditions. We can observe that only the half of the image is covered ².

For each scan-line we create a spatio-temporal image that contains that scan-line in the last 16 frames. The scan-line from the last image is placed at the upper part of the spatio-temporal image and the rest of the scan-lines are shifted to the bottom. The orientation of each scan-line in the spatiotemporal image is defined as follows: the farther/closer point of each scan-line in the image plane is placed on the left/right side of the spatiotemporal image. As can be observed in Figs. 6(e)-6(h) the motion patterns showed by the spatio temporal images between the case of a vehicle approaching and no vehicle approaching are, at first glance, very different in both daytime and nighttime scenarios.

B. Feature selection

Given a set of spatio-temporal images, a new descriptor is here introduced by accounting the number of lines and their

²In countries with left-hand traffic the definition of the scan lines will be symmetric and located at the other side.

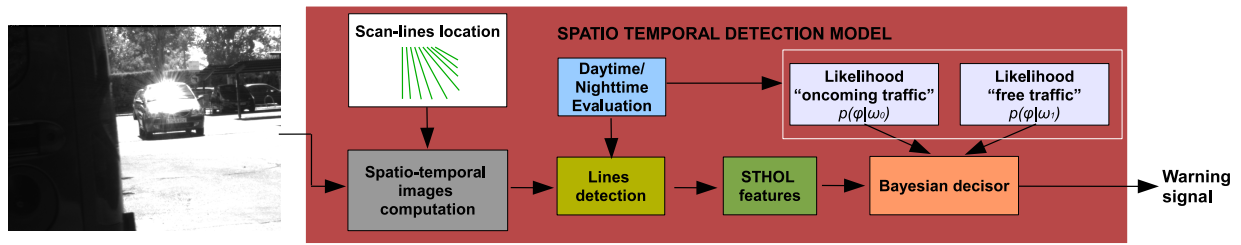


Fig. 5. Overview of the spatio-temporal detection module.

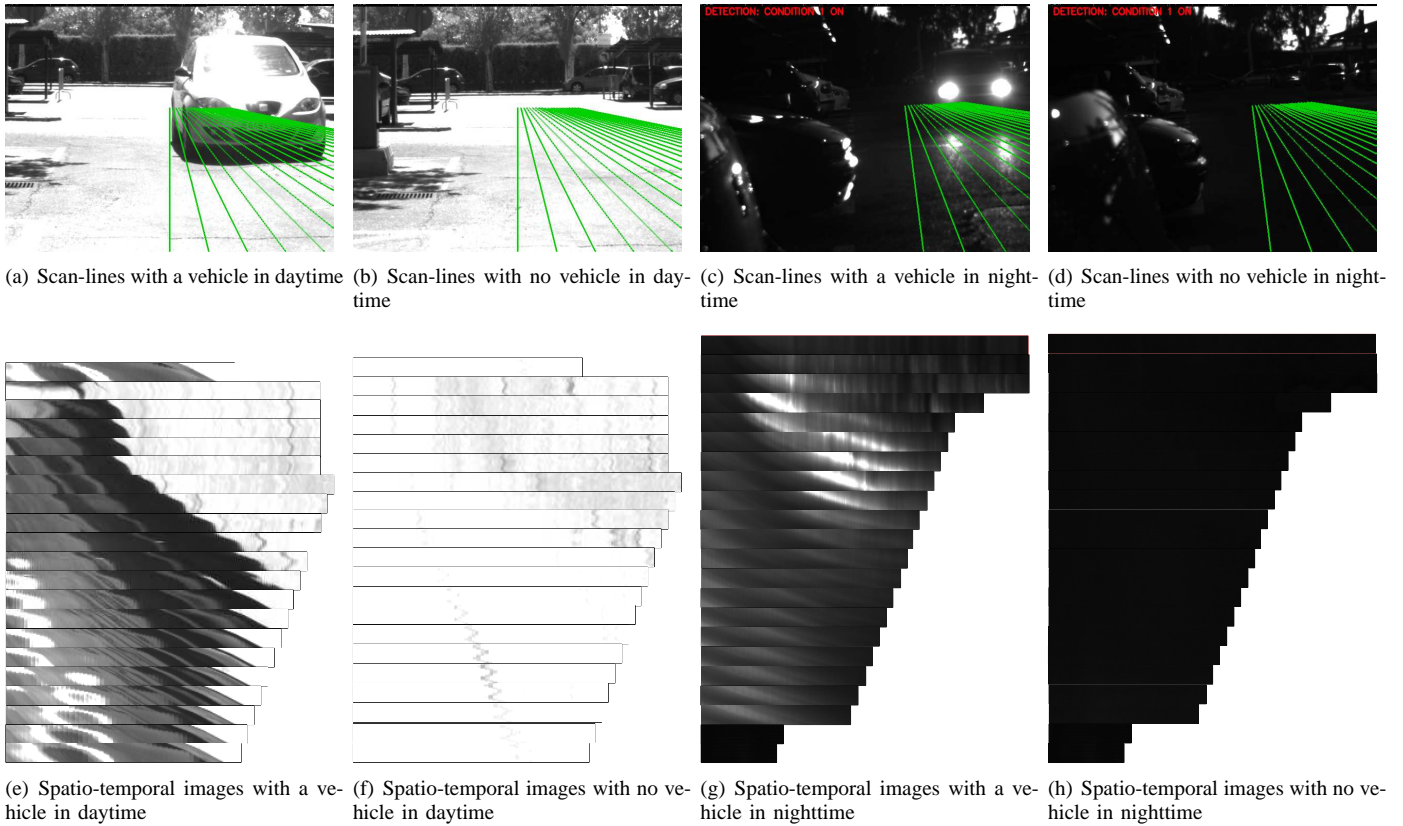


Fig. 6. Two examples of the scan-lines and spatio temporal images. Note that the size of the spatio-temporal images is different depending on the scan-line.

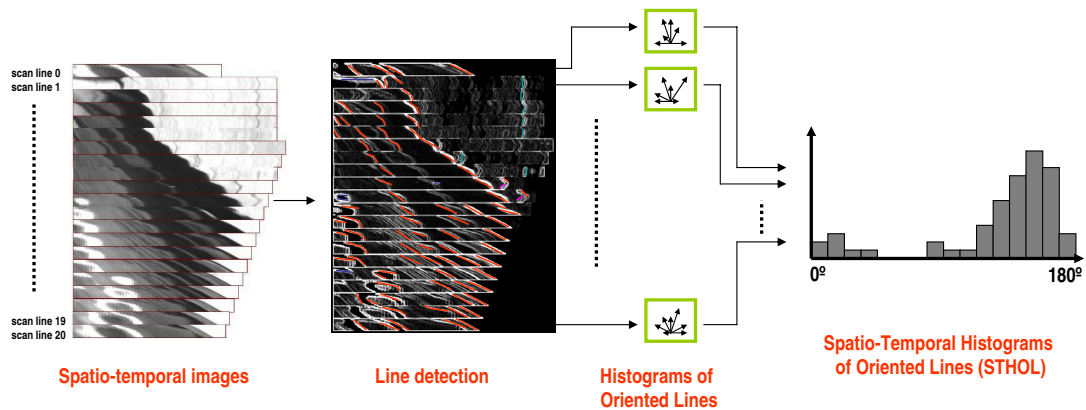


Fig. 7. Overview of the STHOL feature selection architecture.

length with respect to their orientations in a histogram of orientations that we denote as Spatio-Temporal Histograms of Oriented Lines (STHOL). Instead of using the Hough transform as in [12], which in our case provides noisy results, we propose to use the approach suggested by [13]. The first step of the line detection is the computation of the image derivatives using Sobel edge detector. Non-maximum suppression and hysteresis thresholding are then applied as defined by the Canny's edge detector. Upper and lower thresholds are adapted depending on the lighting conditions (daytime/nighttime). The gradient direction of the pixels that have been accepted as edges is then quantized into a set of k ranges (in our case, $k = 16$) where all the edge pixels having an orientation within the specific range fall into the corresponding bin and will be properly labeled. The edge pixels having the same label are then grouped together using connected components algorithm. The line segment candidates are obtained by fitting a line parameterized by an angle θ and a distance from the origin ρ using the following expression:

$$\rho = x \cos \theta + y \sin \theta \quad (1)$$

Each obtained connected component is a list of edge pixels (u_i, v_i) with similar gradient orientation, which is considered as the line support regions. The line parameters are then determined from the eigenvalues λ_1 and λ_2 and eigenvectors \vec{v}_1 and \vec{v}_2 of the matrix D associated with the line support region which is given by:

$$D = \begin{bmatrix} \sum_i (x_i - \bar{x})^2 & \sum_i (x_i - \bar{x})(y_i - \bar{y}) \\ \sum_i (x_i - \bar{x})(y_i - \bar{y}) & \sum_i (y_i - \bar{y})^2 \end{bmatrix} \quad (2)$$

where $\bar{x} = \frac{1}{n} \sum_i x_i$ and $\bar{y} = \frac{1}{n} \sum_i y_i$ are the mid-points of the line segment. The second eigenvalue of an ideal line should be zero. The quality of the lines fit is modeled by the ratio of the two eigenvalues of matrix D , i.e., $\frac{\lambda_1}{\lambda_2}$. Thus a second thresholding procedure is applied in order to reduce the noise of the measurements. The accepted lines will then correspond to clear edges. If the eigenvector \vec{v}_1 is associated with the largest eigenvalue, the line parameters (ρ, θ) are determined using:

$$\begin{aligned} \theta &= \text{atan2}(\vec{v}_1(2), \vec{v}_1(1)) \\ \rho &= \bar{x} \cos \theta + \bar{y} \sin \theta \end{aligned} \quad (3)$$

This procedure is applied on each one of the spatio-temporal images, providing a set of lines with their orientation and length. Motion patterns corresponding to oncoming traffic yield a considerable number of lines with a specific orientation that clearly differs from cases without oncoming vehicles for both daytime and nighttime scenarios (see Figs. 6(e)-6(h)). The number of lines detected on each spatio-temporal image is then combined in an orientation histogram with d bins evenly spaced over 0° - 180° (unsigned gradient, i.e., the sign of the line is ignored). To take into account the strength of each line, votes are directly related with the length of the line in the so-called Histograms of Orientation of Lines (HOL). A similar approach was presented in [14] for rain/snow detection in the so-called Histograms of Orientations of Streaks (HOS),

including uncertainty on the estimation of the orientation of each streak.

Each image, which integrates information from the last 16 frames, provides a specific d -dimensional feature vector that accounts for the number of lines, their lengths and their orientation corresponding to the spatio-temporal images of all the pre-defined scan-lines. We have called this feature vector Spatio-Temporal Histograms of Oriented Lines (STHOL). An overview of the proposed architecture is depicted in Fig. 7.

C. Bayesian decision scheme

Given a particular image I that contains temporal information of the last 16 frames, our aim is to estimate its posterior probability, $P(\omega_0|I)$ with respect to the *oncoming traffic* class ω_0 . To that extend, we represent the image I in terms of STHOL features ϕ_I and follow a Bayesian approach considering the *free traffic* class:

$$P(\omega_0|I) = P(\omega_0|\phi_I) = \frac{p(\phi_I|\omega_0)P(\omega_0)}{\sum_{i=0}^1 p(\phi_I|\omega_i)P(\omega_i)} \quad (4)$$

Although, it may be intuitive to consider the *free traffic* class to be more probable than the *oncoming traffic* class, priors for both *oncoming traffic* ω_0 and *free traffic* ω_1 class, $P(\omega_0)$ and $P(\omega_1)$ are considered uniform and equal. This is an obvious simplification that could be overcome by, for example, modeling the priors using traffic data depending on the time and the global positioning where the vehicle is parked. We consider this interesting analysis out of the scope of this paper. Accordingly, since we manage equal priors, and the evidence $\sum_{i=0}^1 p(\phi_I|\omega_i)P(\omega_i)$ is also common to both classes, our problem can be simplified by estimating and evaluating the likelihoods $p(\phi_I|\omega_i)$ which represent the probability of a particular observation (feature descriptor) given the traffic state of the lane (*oncoming traffic* or *free traffic*).

The following multivariate normal density function is used to model the likelihoods, $p(\phi_I|\omega_i) \sim N(\mu_i, \Sigma_i)$:

$$p(\phi_I|\omega_i) = \frac{1}{(2\pi)^{d/2} |\Sigma_i|^{1/2}} \exp \left[-\frac{1}{2} (x - \mu_i)' \Sigma_i^{-1} (x - \mu_i) \right] \quad (5)$$

where x is the d -component feature descriptor (STHOL), μ_i is the d -component mean vector for class ω_i and Σ_i is the d -by- d covariance matrix corresponding to class ω_i . The next parameters are then estimated using the training data: sample means μ_0 and μ_1 and sample covariance matrices Σ_0 and Σ_1 .

We finally use the minimum-error-rate classification using the discriminant function:

$$g_i(x) = \ln p(\phi_I|\omega_i) + \ln P(\omega_i) \quad (6)$$

By merging Eq. 5 and Eq. 6 we have:

$$g_i(x) = -\frac{1}{2} (x - \mu_i)' \Sigma_i^{-1} (x - \mu_i) - \frac{d}{2} \ln 2\pi - \frac{1}{2} \ln |\Sigma_i| + \ln P(\omega_i) \quad (7)$$

Taking into account that we consider equal priors, and equal feature vector dimension for each class, the terms $(d/2) \ln 2\pi$

and $\ln P(\omega_i)$ can be dropped from Eq. 7, giving the following discriminant function:

$$g_i(x) = -\frac{1}{2}(x - \mu_i)' \Sigma_i^{-1} (x - \mu_i) - \frac{1}{2} \ln |\Sigma_i| \quad (8)$$

Instead of using two discriminant functions g_0 and g_1 , and assigning φ_l to ω_0 if $g_0 > g_1$ we define a single discriminant function $g(x) = g_0(x) - g_1(x)$ and we finally trigger the warning signal if $g(x) > \theta_{TH}$.

V. EXPERIMENTS

The proposed oncoming vehicle detection approach to assist the driver when leaving a perpendicular or angle parking was tested in experiments with data recorded from a real vehicle in real urban traffic conditions. Five different locations have been used, including different levels of visibility due to the size of the side parked vehicles, different camera orientations and different lighting conditions. Datasets were acquired in both daytime and nighttime conditions. Some examples of the different locations and lighting conditions contained in our dataset are depicted in Fig. 8.



Fig. 8. Sample images of the datasets. Upper row: daytime examples. Lower row: nighttime examples.

The experimental data is firstly divided in two datasets: daytime and nighttime datasets. Each dataset is then subdivided in other two datasets: one of them is utilized at a time to learn the probabilistic spatio-temporal model (training dataset). Performance is then evaluated in the remaining dataset (test dataset). To evaluate the quality of the proposed method, we have labeled all the images in two categories: oncoming traffic and free traffic. Note that vehicles that are out of the range of the vision system (50m with our configuration) were labeled as free traffic until they enter in the range of the camera. Table I depicts the number of images of both daytime and nighttime datasets, including the number of images with free traffic conditions, the number of images with oncoming traffic as well as the number of vehicle trajectories (one vehicle usually appears a number of frames which is directly related with its speed). In addition, stationary cars or vehicles moving in opposite direction both appearing inside the range area, are considered as free traffic. The proposed method should be able to distinguish these specific cases.

In our case the number of bins used in the STHOL features has been experimentally fixed to 36. The mean values of the multivariate normal density function as well as their standard deviations (computed as the squared root of the diagonal elements of the covariance matrices) for both oncoming traffic and free traffic classes in daytime and nighttime conditions are

depicted in Figs. 9(a) and 9(b). As can be observed, the mean values of the multivariate Gaussian modeling corresponding to the STHOL features are very different for both oncoming and free traffic classes. The orientations of most of the lines when a vehicle is approaching lie between $120^\circ - 180^\circ$. The STHOL features in nighttime conditions follow the same distribution as in daytime conditions, but with lower histogram values (specially for the case of free traffic conditions).

The performance of the proposed classifier ensembles in terms of ROC curves are depicted in Fig. 10. These curves are obtained by varying the threshold value θ_{TH} of the discriminant function. The results correspond to single-frame classification. Three curves are showed depending on the training and test data sets used in the experiments. As can be observed, for detection rates below 75% the nighttime test data set reports higher detection rates with lower false positive rates. This is mainly due to the fact that the STHOL descriptor for the case of free traffic conditions in nighttime produce a soft response with low histogram values, as depicted in Fig.9(b). Accordingly, the number of false positives given by the classifier remains very low in comparison with daytime samples. It is remarkable the performance level obtained when classifying the nighttime test data set with the classifier trained with the daytime training data set. This result proves the good behavior of the STHOL features for both daytime and nighttime scenarios, as well as the generalization capacity of the proposed detection method.

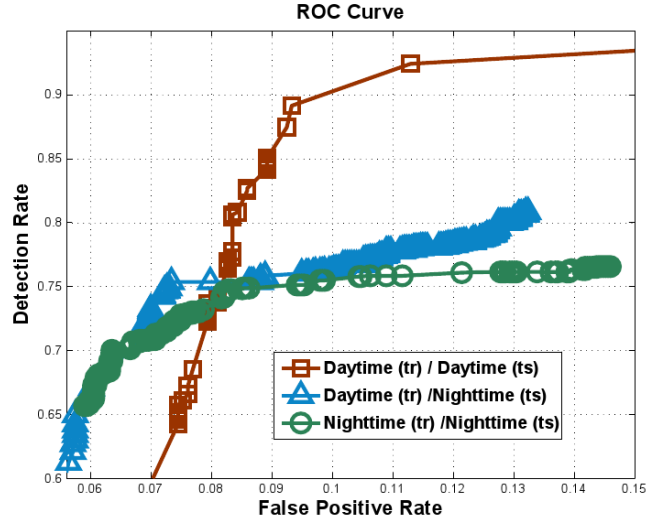


Fig. 10. Receiver-Operating-Characteristic curves of the single frame Bayesian classifiers. We show both daytime and nighttime results, and the results of the classifier trained with the daytime training data set and tested with the nighttime test data set.

After defining the operation point from ROC curves (the threshold value of the discriminant function) for both daytime and nighttime stages, single-frame results are finally integrated in time, using a median filter that considers the last five results. Thus, the system is able to deal with spurious errors, providing a steadier warning signal. Multi-frame results are depicted in Table II. Detection rate of the daytime detection scheme is increased by 17% for a false detection rate of 0.083

TABLE I
STATISTICS OF THE CONSIDERED DATA SETS.

	DAYTIME		NIGHTTIME	
	Training	Test	Training	Test
# of images	16124	6902	9914	4830
# of free traffic images	12862	4838	6597	3166
# of oncoming traffic images	3262	2064	3317	1664
# of vehicle trajectories	34	15	30	14

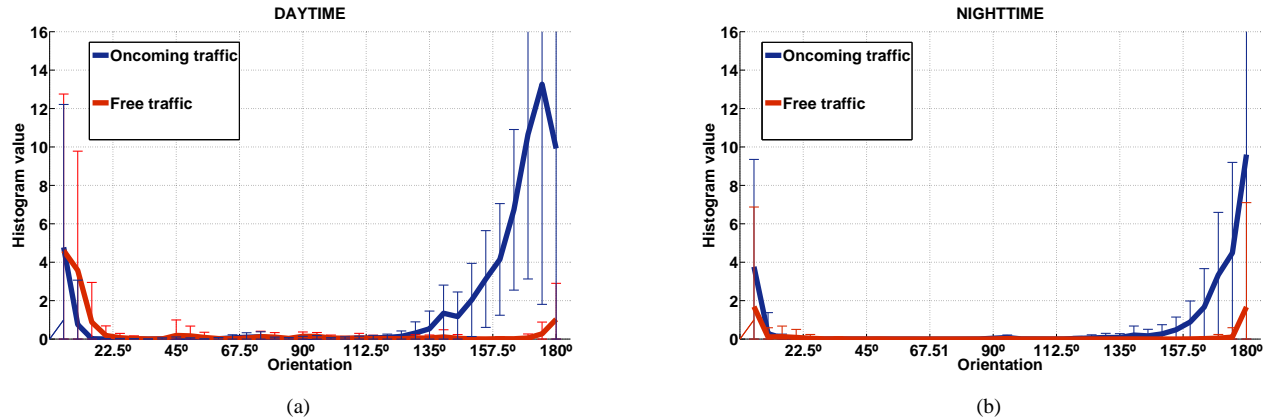


Fig. 9. Mean value of the multivariate Gaussian and standard deviations (square root of the diagonal elements of the covariance matrix) corresponding to both oncoming traffic (blue) and free traffic (red) for (a) daytime and (b) nighttime scenarios.

from single-frame to multi-frame, proving that a considerable number of errors are spurious. However that is not the case of nighttime results, in which detection rate is only improved by 1.3% for a false positive rate of 0.081.

TABLE II
MULTI-FRAME DETECTION RESULTS

	DAYTIME	NIGHTTIME
Detection Rate	0.9596	0.7656
False Positive Rate	0.0830	0.0811
Accuracy	0.9350	0.8615

In order to better show the real performance of the proposed system, Figs. 11(a)-11(b) and 12(a)-12(b) depict the results (single-frame and multi-frame) compared with the ground truth for daytime and nighttime respectively. Test sequences have been joined in one sequence, although we have split each sequence in two for visualization purposes. In addition, some examples of each sequence are overlapped for better understanding. Thus, in Fig. 11(a) first example corresponds to a good detection. Second and third examples correspond to false positives due to near vehicles that finally did not follow the oncoming direction. Both examples of Fig. 11(b) match with correct oncoming traffic detection. Considering nighttime results, in Fig. 12(a) first and third examples correspond to false positives related with far vehicles that finally did change their direction. The problem here is that their headlamps produced overexposure as well as strong reflections of the road surface. On the contrary, this effect produces anticipation in the warning signal in other cases, like the second example of Fig. 12(a). In other words, headlight reflections on the road means false positives but also true positives detected at farther

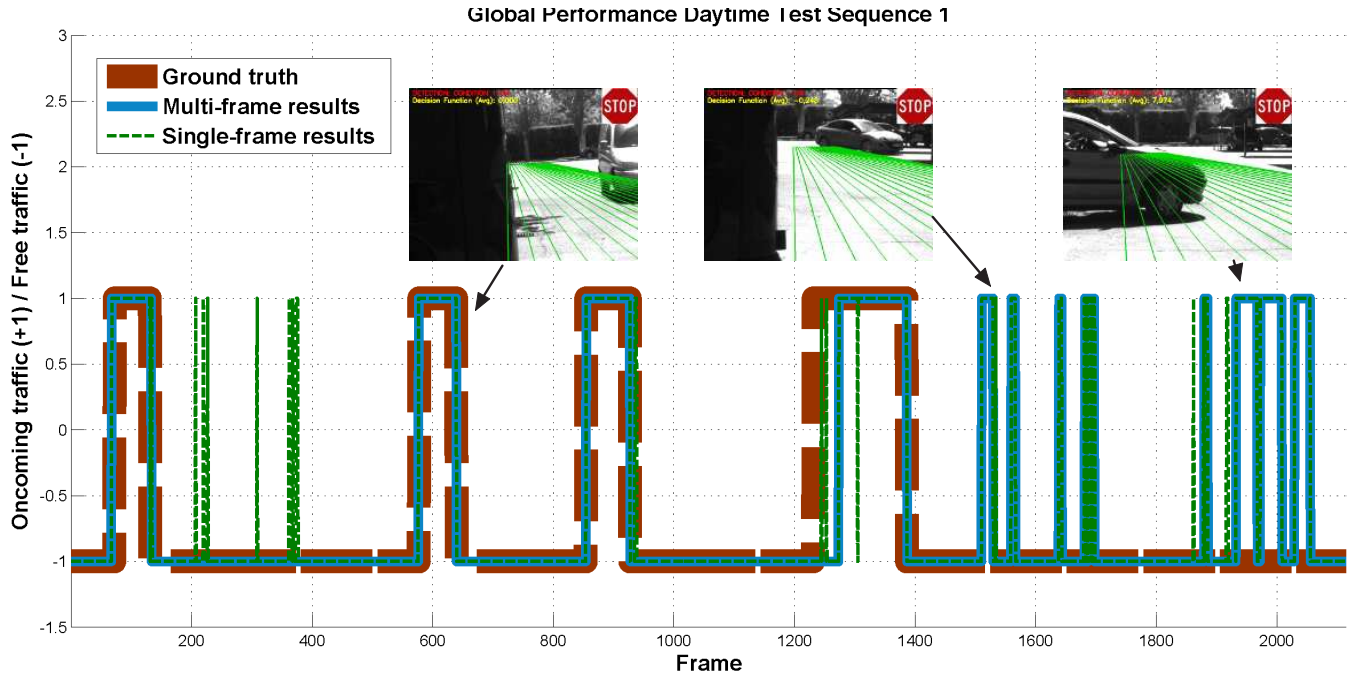
distances. In Fig. 12(b), first and third examples correspond to correct oncoming traffic scenarios. Second example can be considered here as the unique oncoming traffic situation that was not detected by our system. In this specific sequence a very small camera shutter was defined. As can be observed this configuration lead to extremely poor visibility that did not generate contrast in the spatio-temporal images, so that the STHOL descriptor obtained here was close to zero. Headlights are visible and generate contrast, but in this case the headlights did not pass through the grid of scan-lines. Obviously, this is not a good shutter configuration for our approach.

In order to provide a global evaluation of the detection performance of the system, we consider a good detection when the system warns the driver during a sufficient period of time (at least 2 seconds, i.e., around 40 consecutive frames³) when a vehicle is approaching. Accordingly, detection rate is 100% (15/15) and 93% (13/14) for daytime and nighttime conditions respectively. The false negative provided by the system (see Fig. 12(b)) was due to extreme underexposure conditions.

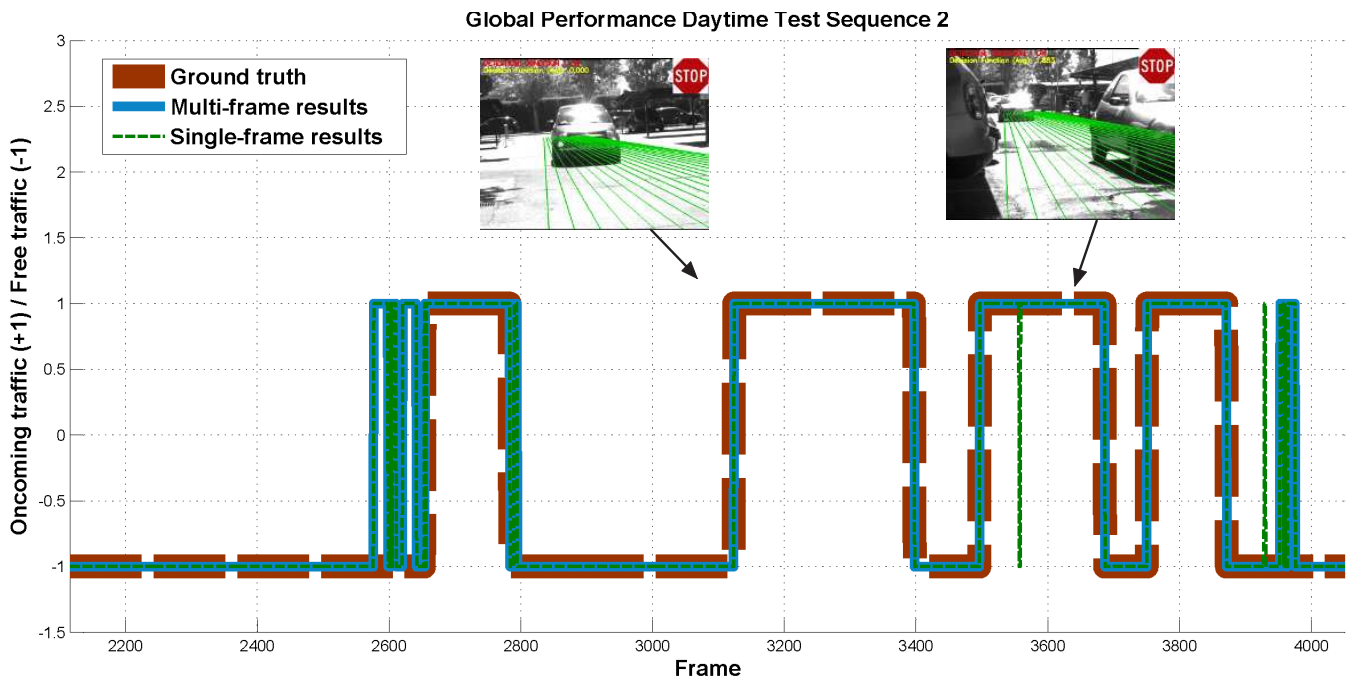
VI. CONCLUSION

This paper presented a novel solution to a new type of ADAS to automatically warn the driver when backing-out in perpendicular or angle parking lots, specially in cases where side parked cars block the driver view of the potential traffic flow. Up to now this is the first approach presented to deal with this specific problem.

³Processing time is around 20Hz using a C/C++ implementation on a state-of-the-art 2.66 GHz Intel PC.

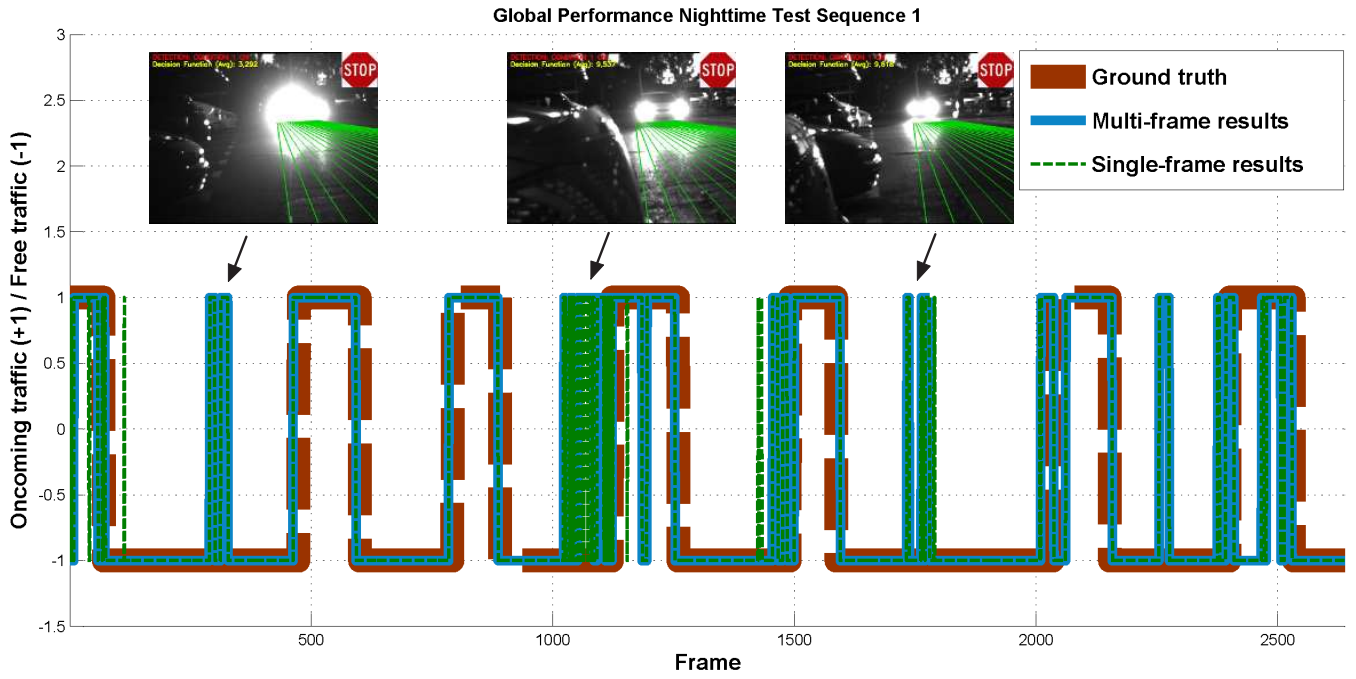


(a)

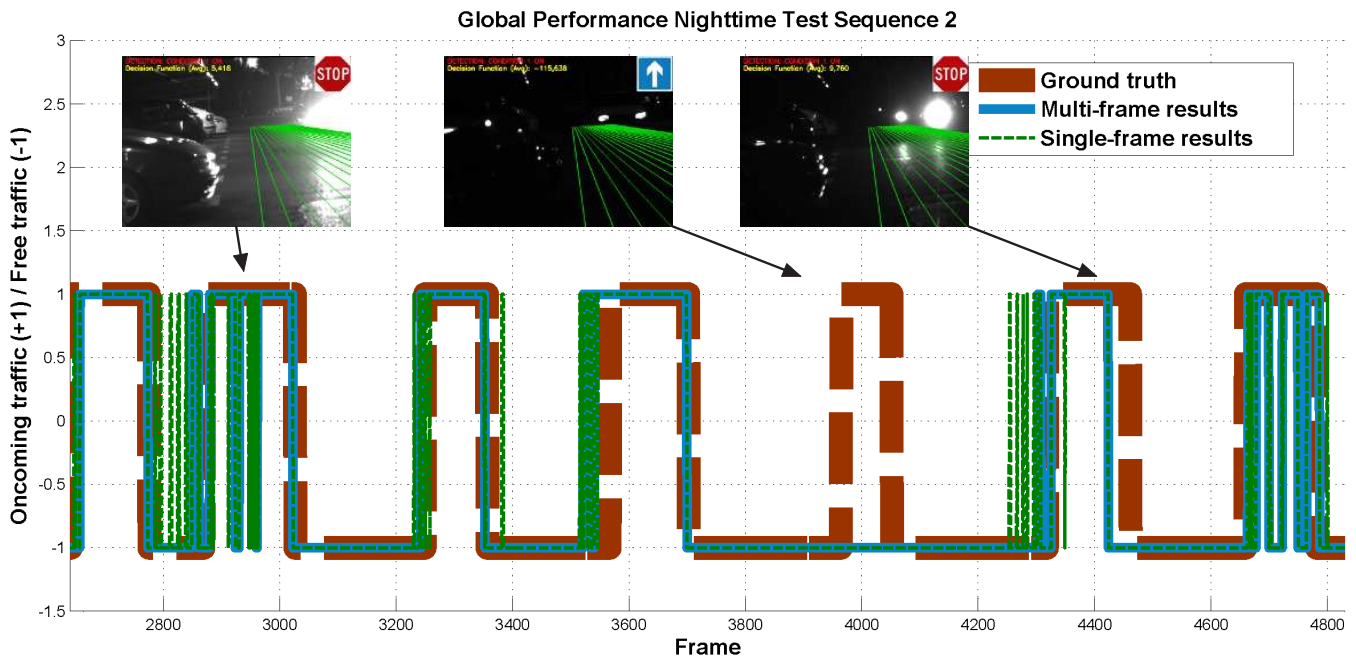


(b)

Fig. 11. Examples of daytime global performance on the test data set. Label “+1” is assigned to oncoming traffic state and label “-1” to free traffic state. Both single-frame and multi-frame system outputs are compared with the ground truth.



(a)



(b)

Fig. 12. Examples of nighttime global performance on the test data set. Label “+1” is assigned to oncoming traffic state and label “-1” to free traffic state. Both single-frame and multi-frame system outputs are compared with the ground truth.

The detection of oncoming traffic is handled by a FSM that includes the user activation as the starting point. A novel spatio-temporal motion descriptor is presented (Spatio-Temporal Histograms of Oriented Lines -STHOL-) to robustly represent oncoming traffic or free traffic states. Spatio-temporal images are obtained from a pre-defined grid of scan-lines related with the road position. From each image lines are detected, including their orientation and length. A histogram of oriented lines is obtained from each spatio-temporal image, and the final STHOL descriptor combine all the histograms. A Bayesian framework is finally used to trigger the warning signal.

The presented approach has been tested with data recorded in real traffic conditions in both daytime and nighttime. One of the main contributions is the use of the same architecture, independently of the lighting conditions. Although some parameters of the system have to be adapted for nighttime scenarios, the classifier ensemble remains exactly as it is for daytime conditions.

Future work will be mainly addressed towards establishing a performance comparison between the proposed automatic warning system and human drivers. A considerable improvement in the reaction time is expected. New experiments will be carried out comparing our generative approach with other discriminative approaches such as SVM-based or NN-based. Considering the STHOL feature vector, the use of the uncertainty on the estimation of line orientation as well as filtering approaches to compute a temporally smoothed model will be studied [14]. In addition, for cases in which global vehicle localization is available, a more sophisticated approach is being planned to model the priors using massive traffic data globally and temporally referenced, since it is obvious that the prior probability of meeting oncoming traffic depends on variables such as the time of the day, the type of road, etc. Finally, more experimental work should be carried out including a more representative data set, optimization procedures and different configurations of the STHOL feature descriptor.

VII. ACKNOWLEDGMENTS

This work was supported by the Spanish Ministry of Science and Innovation under Research Grant ONDA-FP TRA2011-27712-C02-02.

REFERENCES

- [1] NHTSA, "Vehicle backover avoidance technology," National Highway Traffic Safety Administration, Madrid, Spain, Report to Congress, 2006.
- [2] D. F. Llorca, S. Álvarez, and M. A. Sotelo, "Vision-based parking assistance system for leaving perpendicular and angle parking lots," in *IEEE Intelligent Vehicle Symposium*, 2013.
- [3] H. G. Jung, Y. H. Cho, P. J. Yoon, and J. Kim, "Scanning laser radarbased target position designation for parking aid system," *IEEE Trans. on Intell. Transp. Sys.*, vol. 9, pp. 406–424, 2008.
- [4] H. G. Jung, D. S. Kim, P. J. Yoon, and J. Kim, "Parking slot markings recognition for automatic parking assist system," in *IEEE Intelligent Vehicle Symposium*, 2006.
- [5] H. G. Jung, D. S. Kim, and J. Kim, "Light-stripe-projection-based target position designation for intelligent parking-assist system," *IEEE Trans. on Intell. Transp. Sys.*, vol. 11, pp. 942–953, 2010.
- [6] —, "Automatic free parking space detection by using motion stereo-based 3d reconstruction," *Machine Vision and Applications*, vol. 21, pp. 163–176, 2010.

- [7] M. A. Sotelo, J. Barriga, D. Fernández, I. Parra, J. E. Naranjo, M. Marrón, S. Álvarez, and M. Gavilán, "Vision-based blind spot detection using optical flow," *EUROCAST 2007, LNCS*, vol. 4739, pp. 1113–1118, 2007.
- [8] Z. Sun, G. Bebis, and R. Miller, "On-road vehicle detection: A review," *IEEE Trans. on Pattern Analysis and Machine Intelligence*, vol. 28, pp. 694–711, 2006.
- [9] D. Balcones, D. F. Llorca, M. A. Sotelo, M. Gavilán, S. Álvarez, I. Parra, and M. Ocana, "Real-time vision-based vehicle detection for rear-end collision mitigation systems," *EUROCAST 2009, LNCS*, vol. 5717, pp. 320–235, 2009.
- [10] D. F. Llorca, M. A. Sotelo, A. M. Hellín, A. Orellana, M. Gavilán, I. G. Daza, and A. G. Lorente, "Stereo regions-of-interest selection for pedestrian protection: A survey," *Transportation Research Part C*, vol. 25, pp. 226–237, 2012.
- [11] C. Fernández, D. F. Llorca, M. A. Sotelo, I. G. Daza, A. M. Hellín, and S. Álvarez, "Real-time vision-based blind spot warning system: Experiments with motorcycles in daytime/nighttime conditions," *International Journal of Automotive Industry*, vol. 14, pp. 113–122, 2013.
- [12] P. Reisman, O. Mano, S. Avidan, and A. Shashua, "Crowd detection in video sequences," in *IEEE Intelligent Vehicle Symposium*, 2004.
- [13] W. Zhang and J. Kosecka, "Efficient computation of vanishing points," in *IEEE International Conference on Robotics and Automation*, 2002.
- [14] J. Bossu, N. Hautière, and J.-P. Tarel, "Rain or snow detection in image sequences through use of a histogram of orientation of streaks," *International Journal of Computer Vision*, vol. 93, pp. 348–367, 2011.